

Article

Rapid Urbanization Has Changed the Driving Factors of Groundwater Chemical Evolution in the Large Groundwater Depression Funnel Area of Northern China

Long Wang, Qianqian Zhang * and Huiwei Wang

Hebei and China Geological Survey Key Laboratory of Groundwater Remediation, Institute of Hydrogeology and Environmental Geology, Chinese Academy of Geological Sciences, Shijiazhuang 050061, China

* Correspondence: zhangqianqian@mail.cgs.gov.cn

Abstract: With the rapid development of urbanization, the chemical evolution of groundwater has been significantly affected by human activities. However, the driving mechanisms of groundwater chemical evolution at different stages of urbanization are still unclear, which severely affects the implementation of groundwater protection. This study investigated the driving mechanisms of groundwater chemical evolution based on the long-term series (from 1985 to 2015) of hydrochemical data from 19 groundwater monitoring sites in rapidly urbanizing areas (Shijiazhuang, Hebei Province, China). The results show that the concentrations of various chemical components in groundwater gradually increase with the acceleration of the urbanization process, especially NO_3^- , which has increased from 13.7 mg/L in the primary stage of urbanization (PSU) to 65.1 mg/L in the advanced stage of urbanization (ASU), exceeding the World Health Organization (WHO) drinking water standard (50 mg/L), indicating that the groundwater chemistry has been significantly affected by human activities. The main hydrochemical types have changed from the $\text{HCO}_3\text{-SO}_4\text{-Ca}\cdot\text{Mg}$ -type water in the primary stage of urbanization (PSU) to the $\text{SO}_4\cdot\text{HCO}_3\text{-Ca}\cdot\text{Mg}$ -type water in the advanced stage of urbanization (ASU). It is worth noting that there are obvious differences in driving factors of groundwater chemical evolution at different urbanization stages. In the primary stage of urbanization (PSU), the driving factors were carbonate and rock salt dissolution, cation exchange, and industrial activities. However, in the intermediate stage and advanced stage, the driving factors were changed to carbonate and gypsum dissolution, groundwater over-exploitation, agricultural fertilization, and domestic sewage. Based on the above conclusions, it is suggested that future groundwater management should control the amount of agricultural fertilizers, apply scientific fertilization, and prohibit the discharge of various types of non-compliant sewage, while strengthening the supervision of groundwater extraction to reduce the impact of urbanization development on the groundwater chemical evolution process.



Citation: Wang, L.; Zhang, Q.; Wang, H. Rapid Urbanization Has Changed the Driving Factors of Groundwater Chemical Evolution in the Large Groundwater Depression Funnel Area of Northern China. *Water* **2023**, *15*, 2917. <https://doi.org/10.3390/w15162917>

Academic Editor: Dimitrios E. Alexakis

Received: 23 June 2023

Revised: 5 August 2023

Accepted: 10 August 2023

Published: 12 August 2023

Keywords: urbanization; groundwater chemistry; water–rock interaction; multivariate statistical analysis; driving mechanisms

1. Introduction

Groundwater, as an essential component of water resources, plays a vital role in maintaining ecological balance, ensuring residents' livelihoods, and supporting socio-economic development [1–6]. The variation of chemical components in groundwater has significant impacts on water quality and human health, making it extremely important to understand the hydrochemical evolution process of groundwater thoroughly [7].

Groundwater chemical evolution is mainly controlled by anthropogenic activities (sewage discharge, agricultural fertilizer, mining operations, etc.) and natural factors (aquifer lithology, soil characteristics, groundwater–rock interaction, etc.) [8–10]. For example, researchers discovered that the $\text{HCO}_3\text{-Cl}$ -type, Cl-HCO_3 -type, and NO_3 -type waters frequently appear under the influence of human activities, making groundwater



Copyright: © 2023 by the authors. Licensee MDPI, Basel, Switzerland. This article is an open access article distributed under the terms and conditions of the Creative Commons Attribution (CC BY) license (<https://creativecommons.org/licenses/by/4.0/>).

chemistry more diverse and complex [11]. The combined sewage system (collecting surface runoff and sewage water in a shared system simultaneously) could accelerate the effects of sewage on groundwater chemistry [12]. Additionally, researchers have found that socio-economic development and land use types also have important impacts on the evolution of groundwater chemistry [13,14]. Nowadays, with the rapid development of urbanization and industrialization processes, the influence of human activities on the chemical evolution of groundwater increased year by year [15–17], and the driving mechanism of groundwater chemical evolution may have changed. However, previous studies mainly discussed the controlling factors of groundwater chemical evolution on the same time scale, but the impact of different urbanization stages on the groundwater chemical evolution has not yet been reported. This seriously limits the implementation of groundwater protection in different urbanization areas.

To fill this research gap, we selected a typical area strongly affected by human activities which experienced rapid urbanization—the Shijiazhuang section of Hutuo River alluvial fan (the largest groundwater funnel area in the North China Plain) [18,19]—as our study area. Based on the long-term series data (over 30 years) from 19 groundwater sites, we focused on discussing the driving mechanisms of groundwater chemical evolution at different stages of urbanization. The objectives of this study are the following: (1) to analyze the impact of urbanization development on groundwater components and hydrochemical types; (2) to identify the influence mechanisms of natural factors and human activities on the hydrochemical evolution of groundwater at different stages of urbanization; and (3) to reveal the driving factors of groundwater chemical evolution at different stages of urbanization through the principal component analysis (PCA). The results can provide an important reference for the study of groundwater chemical evolution in areas that have not yet experienced rapid urbanization and provide a scientific basis for the protection of groundwater in different urbanizing areas.

2. Study Area

2.1. General Setting

The Shijiazhuang section of the Hutuo River alluvial fan (with an area of about 1500 km²) is located in the piedmont inclined plain area at the eastern foot of Taihang Mountain in Hebei Province, China (Figure 1). The study area has a permanent population of approximately 5.2 million and a cultivated land area of about 60 × 10⁴ hm². This region has distinct seasons and belongs to a semi-humid and semi-arid continental monsoon climate. The average annual precipitation is about 550 mm/yr which is unevenly distributed over time, mainly concentrating between April and September, accounting for 70% to 80% of the annual precipitation. The annual evaporation ranges from 1600 mm/yr to 2100 mm/yr, and the average annual temperature is 13.0 °C [20].

Based on the urbanization rate (the urban population accounts for the proportion of the total population), the study area was divided into three stages of urbanization. The first stage (1985~1995) is the primary stage of urbanization (PSU) (the number of samples is 57), with an urbanization rate less than 30.0%; the second stage (1986~2005) is the intermediate stage of urbanization (ISU) (the number of samples is 57), with an urbanization rate between 30.1% and 50.0%; and the third stage (2006~2015) is the advanced stage of urbanization (ASU) (the number of samples is 38), with an urbanization rate between 50.1% and 75.0%.

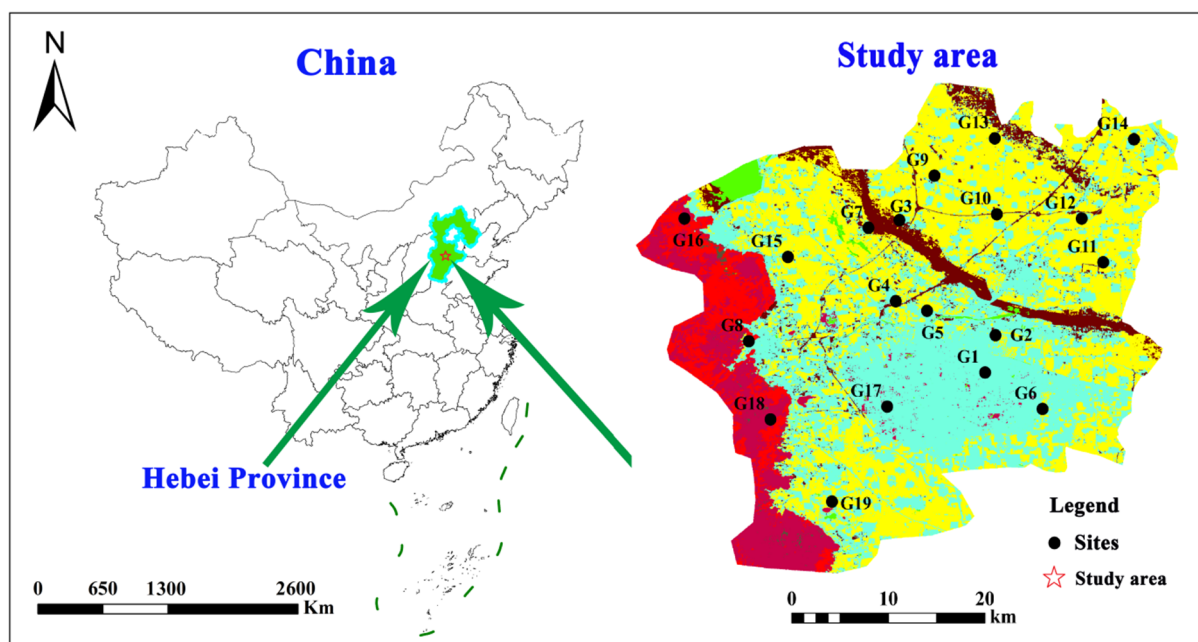


Figure 1. Distribution map of groundwater sample sites.

2.2. Geological and Hydrogeological Conditions

The strata in the study area are primarily composed of Quaternary sediments, and the lithology mainly consists of clay loam, sandy loam, sandy-silty clay, and gravel and sand layers of different particle sizes. The lithology of Quaternary sediments is mainly composed of clayey loam, sandy loam, sand-bearing clayey loam and pebbles, gravel, and sand layers of different particle sizes. The sediments came from the western Taihang Mountains and were mainly transported by the Hutuo River. Quaternary stratigraphic lithology includes lower Pleistocene (Q_1), Middle Pleistocene (Q_2), Upper Pleistocene (Q_3) and Holocene (Q_4). The stratigraphic lithology of Q_1 is mainly composed of medium-coarse sand, medium-fine sand, and clay and clay loam with a thickness of 200–300 m. The stratigraphic lithology of Q_2 is mainly composed of sandy gravel, pebbles, medium-coarse sand, and part of medium-fine sand with clayey loam and sand-bearing clayey loam, and its thickness of 50–80 m. The formation lithology of Q_3 is mainly composed of sandy loam, clay loam and sand bed, and sand gravel, with the thickness of 50–70 m. Q_4 is mainly composed of sandy loam, silty sand and part of sandy gravel, and clay loam, with a thickness of 5–20 m.

The main aquifer in the study area belongs to the Quaternary super-thick, multi-layer aquifer system in the Hebei Plain, China. Groundwater mainly occurs in the strata of Upper Pleistocene and Lower Pleistocene, and the aquifer lithology mainly includes sand gravel, coarse sand with gravel, and medium sand. The water table depth ranges from 12 to 240 m, and the aquifer thickness is between 20 and 140 m, both showing good conductivity and water yield. Shallow groundwater is mainly supplied by atmospheric precipitation infiltration, lateral runoff, surface water infiltration, and agricultural irrigation return flow, among which atmospheric precipitation infiltration is the primary recharge method. Discharge is mainly through artificial extraction, followed by lateral runoff. Deep groundwater flows from the northwest to the southeast, mainly recharged by lateral runoff, and is discharged through lateral runoff and artificial extraction. Long-term severe over-extraction has led to the formation of the largest falling funnel in the North China Plain in the study area, which also affected the groundwater chemical evolution.

3. Materials and Methods

3.1. Data Sources

Groundwater samples were obtained from eight field surveys conducted during the dry season between 1985 and 2015. The samples consisted of nineteen regular groundwater monitoring stations (the total number of samples is 152). Samples were collected by pumping groundwater from the wells and storing it in one 1.5 L high-density polyethylene sampling bottle for analyzing the hydrochemical parameters. Before taking the samples, the bottle was rinsed 3 times with groundwater at the sampling site. Before collecting samples, these wells were purged for 5–10 min until the pH of the groundwater was stable. The untreated samples were used for anion analysis, while those used for cation analysis were acidified with HCl to $\text{pH} < 2$. All the samples were then stored in the icebox at $4\text{ }^{\circ}\text{C}$ prior to further analysis.

The hydrochemical indicators include pH, potassium (K^+), sodium (Na^+), calcium (Ca^{2+}), magnesium (Mg^{2+}), chloride (Cl^-), sulfate (SO_4^{2-}), bicarbonate (HCO_3^-), nitrate (NO_3^-), total dissolved solids (TDS), and total hardness (TH). pH was measured in situ using portable electrodes. The anions were measured using a spectrophotometer, while the cations were determined using an inductively coupled plasma-emission spectrometer. TH was measured by the ethylene–diamine–tetraacetic acid (EDTA) titration method. Details of the analytical parameters, methods and detection limits are presented in Supplementary Table S1.

The quality assurance and quality control (QA/QC) for analysis strictly followed the guidelines set by the methods for examination of drinking natural mineral water in China (GB/T8538-2008) [21].

3.2. Data Analysis

In this study, Piper trilinear diagrams are used to interpret water chemical types (the chemical types of groundwater are named according to Shukarev classification) [11] and their variation characteristics. Gibbs diagrams, ion ratio analysis, and principal component analysis (PCA) are used to identify the main controlling factors of water chemical changes.

PCA is a very powerful technique applied to reduce the dimensionality of a dataset consisting of a large number of interrelated variables, while retaining as much as possible the variability presented in the dataset. Before inputting the data into the model, Kaiser–Meyer–Olkin and Barlett’s sphericity tests were performed on the research data. The results showed that the KMO values were 0.502, 0.454, and 0.621 for the three urbanization stages and Barlett’s sphericity test values were 820, 1272, and 468 ($p < 0.001$), respectively, indicating that the water chemistry data met the requirements of PCA. In our study, the normalized variables (groundwater parameters dataset) were performed to extract the significant principal components and further reduce the contribution of variables with minor significance. These PCs were subjected to varimax rotation (raw) to generate original variables. Following this, eigenvalues >1 were selected as the new orthogonal variables. According to the literature, the factor loadings of “strong”, “moderate”, and “weak” correspond to the absolute loading values of >0.75 , $0.75\text{--}0.50$, and $0.50\text{--}0.30$, respectively [22].

Data analysis and processing were carried out using SPSS 21 (SPSS Inc., Chicago, IL, USA), Origin 2022, and ArcGIS 10.5 software (ESRI Inc., Redlands, CA, USA).

4. Results and Discussion

4.1. Analysis of Groundwater Chemical Composition Characteristics

4.1.1. pH

The pH of groundwater in the study area ranges from 7.18 to 8.20, with an average of 7.56, and shows a neutral to weak alkaline water. This is closely related to the formation lithology (limestone is the main rock type in this area) and the over-extraction of groundwater (which results in more salt-based ions being present in groundwater) [23]. The pH fluctuations of different monitoring stations within different urbanization stages are

small, meeting the WHO drinking water standard (between 6.5 and 8.5) [24]. The average pH values for the three development stages (PSU, ISU, and ASU) are 7.56, 7.52, and 7.50, respectively, showing no significant changes. Meanwhile, there is an inverse relationship between pH and major cation concentrations (Figure 2). This may be related to the carbon dioxide emissions from industrial and agricultural activities entering groundwater through precipitation infiltration, leading to a decrease in the pH value and an increase in cation concentration.

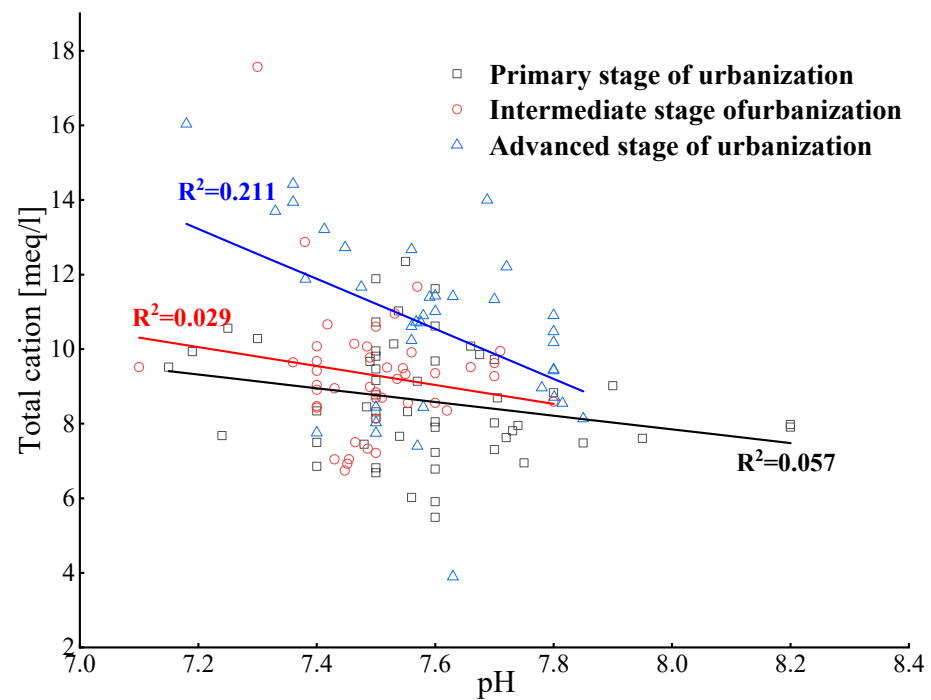


Figure 2. Relationship between pH and the total cations in groundwater.

4.1.2. Ion Characteristics Analysis

We analyzed the characteristics of the primary ion components in groundwater during the three urbanization stages based on a semi-logarithmic plot (Figure 3) and Supplementary Table S2. As seen in Figure 3, the concentration of major ions in groundwater increases with urbanization, and reaches the highest value during the AUS. This indicates that frequent human activities have a strong impact on the chemical composition of groundwater [25]. During the PSU, ISU, and ASU, the Ca^{2+} concentrations are 103 mg/L, 114 mg/L, and 128 mg/L, respectively, all exceeding the WHO water quality standard [26]. This may be related to the lithology of the strata in the study area and long-term over-extraction [27]. In addition, the concentrations of TH (485 mg/L) and NO_3^- (65.1 mg/L) in the ASU also exceed the WHO water quality standard. The high concentration of TH is mainly due to the continuous increase in Ca^{2+} and Mg^{2+} concentrations, while the excessive NO_3^- level is mainly related to human activities [28]. Previous studies have found that NO_3^- in groundwater in the Hutuo River Basin mainly comes from domestic sewage and chemical fertilizers [14].

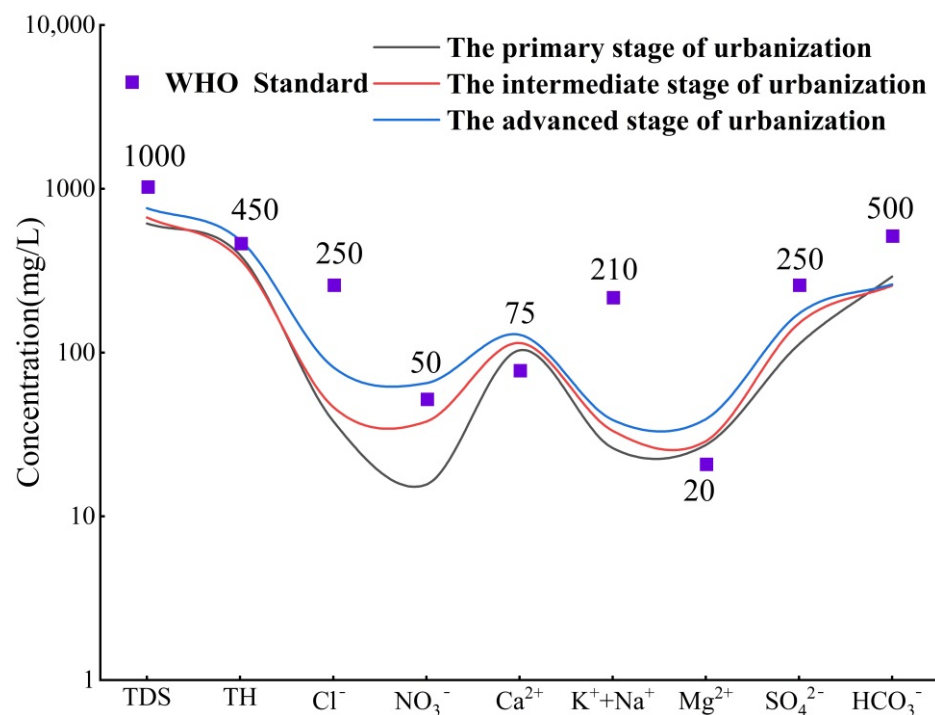


Figure 3. Characteristics of changes in the major chemical components of groundwater.

4.2. Hydrochemical Type Analysis

Based on the Piper trilinear diagrams, we studied the hydrochemical types of groundwater in this area. The three results show that the main hydrochemical type of groundwater in the study area is $\text{HCO}_3 \bullet \text{SO}_4 \text{-Ca} \bullet \text{Mg}$ (Figure 4). During the PUS, the hydrochemical types were mainly $\text{HCO}_3 \bullet \text{SO}_4 \text{-Ca} \bullet \text{Mg}$ or $\text{HCO}_3 \text{-Ca} \bullet \text{Mg}$, accounting for 98.3%, while the rest were of the $\text{SO}_4 \bullet \text{HCO}_3 \text{-Ca}$ type. During the IUS, $\text{HCO}_3 \bullet \text{SO}_4 \text{-Ca} \bullet \text{Mg}$ and $\text{HCO}_3 \text{-Ca} \bullet \text{Mg}$ accounted for 86.0% of the total water samples, and there was a significant decrease compared to the previous stage. A total of 14.0% of water samples were of the $\text{SO}_4 \text{-Ca} \bullet \text{Mg}$ or $\text{SO}_4 \text{-Ca}$ type in the IUS. For the AUS, the proportion of $\text{HCO}_3 \bullet \text{SO}_4 \text{-Ca} \bullet \text{Mg}$ or $\text{HCO}_3 \text{-Ca} \bullet \text{Mg}$ decreased to 73.7%, the $\text{SO}_4 \text{-Ca} \bullet \text{Mg}$ type accounted for 15.8%, and an additional 10.5% of $\text{Cl} \bullet \text{HCO}_3 \bullet \text{SO}_4 \text{-Ca} \bullet \text{Mg}$ -type water appeared. It can be seen that different patterns of hydrochemical types are presented at different levels of urbanization. This changing trend is mainly due to the fact that during the PSU, the hydrochemical types of groundwater in the study area are less affected by human activities and are mainly controlled by the characteristics of the strata. However, in the AUS, when the socio-economic development accelerated, the water demand for the industrial and agricultural industries increased sharply, along with the shortage of surface water sources, which lead to severe over-extraction of groundwater. In addition, the non-compliant discharge of domestic and industrial wastewater causes an increase in the concentration of major ions in the groundwater and results in a change in hydrochemical types [29]. It can be seen that the impact of human activities on the hydrochemistry of groundwater gradually increases with the rapid development of urbanization and industrialization, resulting in a diversified and complex trend of hydrochemical types.

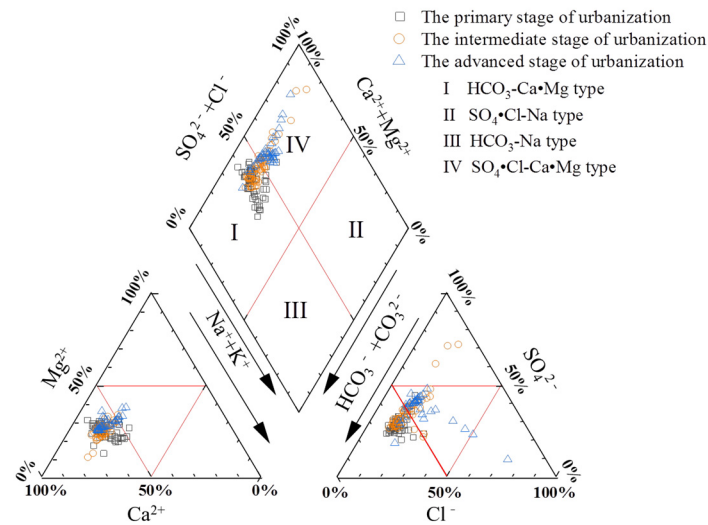


Figure 4. Piper trilinear diagram of groundwater in different stages of urbanization.

4.3. Factors Driving Hydrochemical Evolution

4.3.1. Analysis of Controlling Factors Based on Gibbs Diagram

Rock weathering, precipitation, and evaporation control the changes in natural water chemical components. In this study, a Gibbs diagram was used to analyze the main controlling factors of hydrochemical evolution in the three urbanization stages of the study area. As shown in Figure 5a,b, the groundwater sample points in the three urbanization stages are mainly distributed in the rock differentiation zone, indicating that rock weathering is the main controlling factor of the hydrochemistry in the study area. However, the Gibbs diagram can only explain the natural factors controlling groundwater composition qualitatively but cannot distinguish the influence of human activities. As Section 4.2 shows, in recent years, with the rapid development of the economy, human activities have caused variations in the hydrochemical types of the study area, which will inevitably affect the controlling factors of its hydrochemistry.

4.3.2. Water–Rock Interactions

The source of groundwater chemistry components was identified (carbonates, silicates, and evaporites) through the relationship between $\text{Ca}^{2+}/\text{Na}^+$ and $\text{Mg}^{2+}/\text{Na}^+$ molar ratios [30,31]. As shown in Figure 6a, groundwater samples from the three urbanization stages mainly fall within the carbonate and silicate weathering control zones, indicating that the cations and bicarbonate anions in the water bodies of the study area mainly come from carbonate and silicate weathering dissolution.

By calculating the ratio of Na^+ and Cl^- in groundwater, we further determined the main hydrochemical processes and ion sources. As shown in Figure 6b, Na^+ and Cl^- in water samples from different urbanization stages show a positive correlation, which suggests that Na^+ and Cl^- may have a common source (such as halite dissolution). For the PSU, ISU, and ASU, 56%, 70%, and 68% of water sample points fall above the $y = x$ line, indicating that Na^+ in groundwater comes not only from halite dissolution but also from carbonate and silicate weathering dissolution or cation exchange [32].

Based on the equivalent ratio of $[\text{Ca}^{2+} + \text{Mg}^{2+}]$ and $[\text{HCO}_3^- + \text{SO}_4^{2-}]$, the influence of carbonates and silicates on the formation of water chemical components can be distinguished (Figure 6c). Water samples from the PSU, ISU, and ASU mainly fall above the $y = x$ line, with proportions of 70%, 79%, and 94%, respectively. This indicates that carbonate weathering plays a dominant role in hydrochemical formation during these urbanization stages, and the effect increases gradually with the improvement in urbanization level. The reason may be that the intensification of groundwater exploitation has caused changes in the groundwater dynamic field [33] and increased the time and distance of groundwater

runoff. Therefore, there were more carbonate mineral components and the pollutants generated from human activities entered into groundwater. According to the ratio diagram of Ca^{2+} and SO_4^{2-} (Figure 6d), except for the two water sample points below the $y = x$ line in the ASU, the remaining water samples are above the $y = x$ line. Ion concentrations show an increasing trend at different urbanization stages, but the correlation between Ca^{2+} and SO_4^{2-} is not significant, indicating that they are not from the same source. In addition, Ca^{2+} may also be affected by carbonate and silicate weathering dissolution and reverse cation exchange.

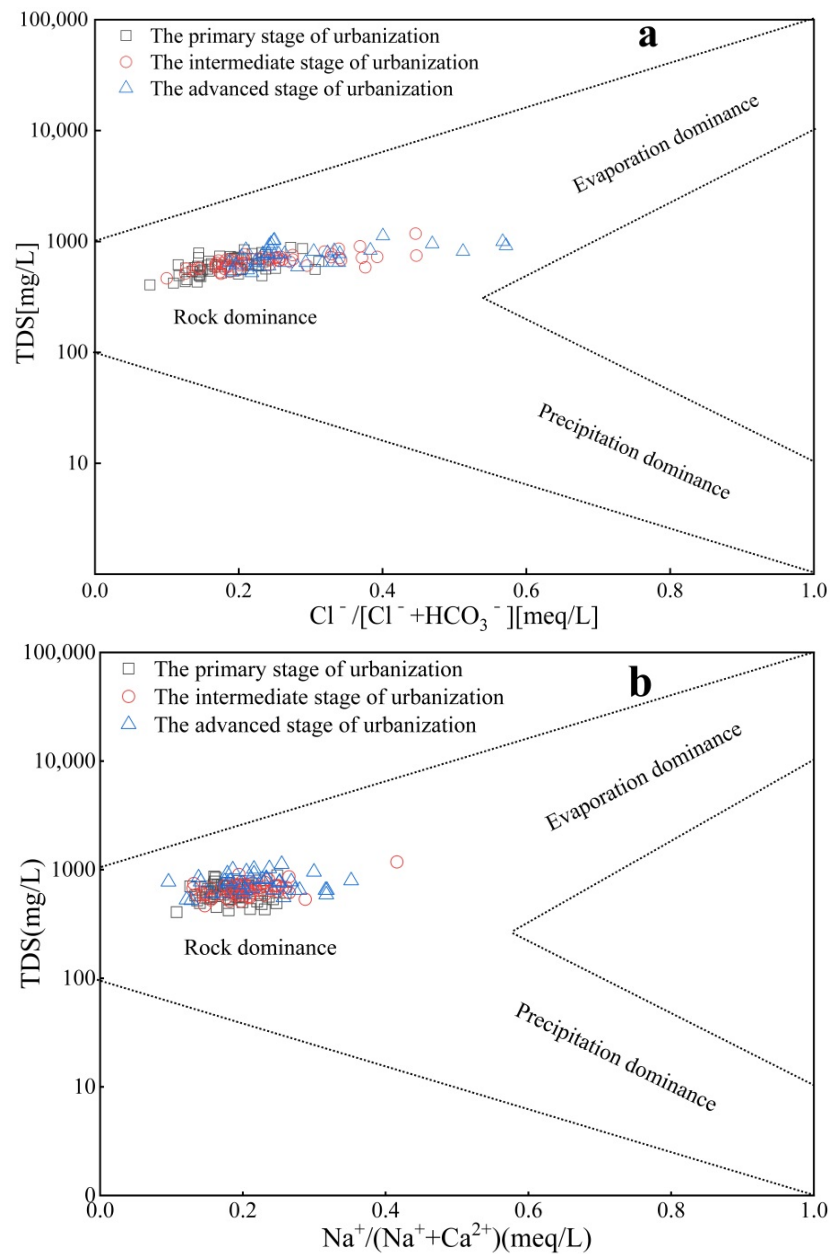


Figure 5. Gibbs diagrams for groundwater in different stages of urbanization ((a) $\text{Cl}^- / [\text{Cl}^- + \text{HCO}_3^-]$ vs. TDS; (b) $\text{Na}^+ / [\text{Na}^+ + \text{Ca}^{2+}]$ vs. TDS).

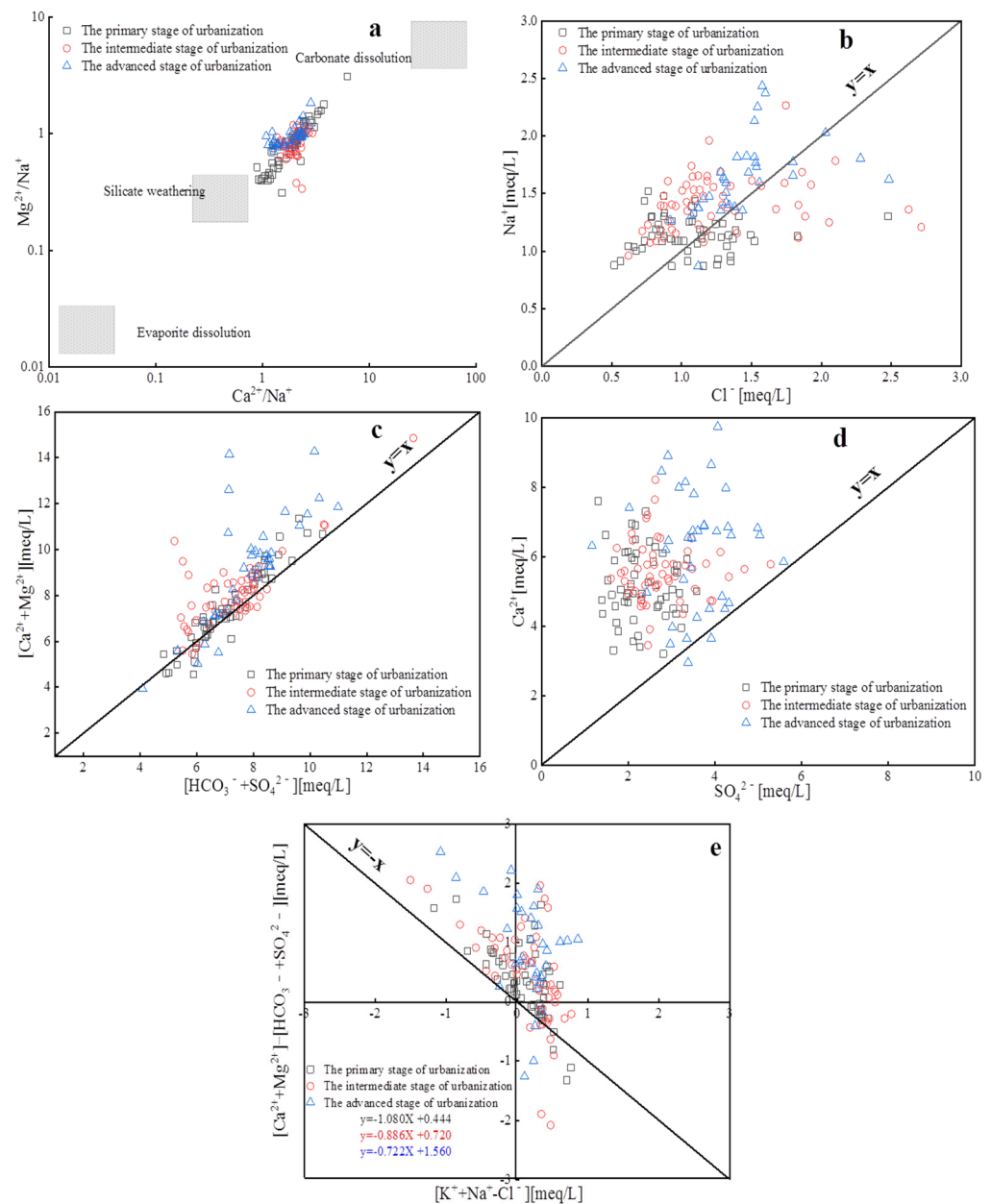


Figure 6. Relationships between major ions for groundwater samples in different stages of urbanization (a) (Ca^{2+}/Na^+) vs. (Mg^{2+}/Na^+) ; (b) Cl^- vs. Na^+ ; (c) $[Ca^{2+} + Mg^{2+}]$ vs. $[HCO_3^- + SO_4^{2-}]$; (d) SO_4^{2-} vs. Ca^{2+} ; (e) $[Na^+ + K^+ - Cl^-]$ vs. $[Ca^{2+} + Mg^{2+} - HCO_3^- - SO_4^{2-}]$.

As mentioned above, cation exchange may have a significant impact on the hydrochemical components of groundwater in the study area. The relationship between $[Na^+ + K^+ - Cl^-]$ and $[Ca^{2+} + Mg^{2+}] - [HCO_3^- + SO_4^{2-}]$ was used to demonstrate the effect. If they exhibit a linear relationship with a slope close to -1 , it indicates that cation exchange is an essential mechanism in the groundwater chemical evolution process.

As shown in Figure 6e, 44%, 30%, and 31% of water sample points fall in quadrant II during each stage, indicating that reverse cation exchange occurs between Na^+ in groundwater and Ca^{2+} and Mg^{2+} in soil/rock at these sites. A total of 24%, 28%, and 14% of water sample points fall in quadrant IV, indicating positive cation exchange between Ca^{2+} and Mg^{2+} in groundwater and Na^+ in soil/rock. Additionally, 31%, 42%, and 55% of water sample points fall in quadrant I during the three urbanization stages, indicating that ion exchange is not the only factor determining Ca^{2+} , Mg^{2+} , and Na^+ content in groundwater. From the results, it can be seen that during the PSU and ISU, cation exchange can be consid-

ered an essential mechanism for hydrochemical action in the study area. However, during the ASU, the proportion of water sample points falling in quadrants II and IV decreases, and the slope of the regression equation ($k = -0.722$) increases, indicating that the influence of cation exchange on the groundwater evolution process has diminished. The reason for this temporal change is related to the relatively stable groundwater environment and slow infiltration rate in the early stages, which provides favorable conditions for cation exchange. However, with the development of social economy, the original groundwater environment has been destroyed, and the emergence of descending funnels has accelerated the seepage velocity of groundwater [23], resulting in the predominance of the leaching effect. At the same time, the return water from agricultural irrigation will also have a vital impact on the water chemistry [34].

4.3.3. Impact of Human Activities on Groundwater Chemical Composition

The influence of human activities on groundwater chemical composition during urbanization stages was studied using the relationship between $\text{NO}_3^-/\text{Na}^+$ and $\text{SO}_4^{2-}/\text{Na}^+$ ratios. As can be seen from Figure 7, during the PSU, ISU, and ASU, the ratios of $\text{NO}_3^-/\text{Na}^+$ are 0.140 to 1.32, 0.160 to 1.33, and 0.320 to 1.26, respectively, while those of $\text{SO}_4^{2-}/\text{Na}^+$ are 1.13 to 5.00, 0.670 to 2.37, and 0.850 to 4.11. The distribution of water samples on the graph indicates that both ratios show an overall increasing trend, but the main controlling factors are different. In the PSU, the groundwater chemistry in the study area is mainly affected by industrial activities, while in the ISU and ASU, the groundwater is jointly affected by industrial and agricultural activities (circled areas in Figure 7), and the influence of agricultural activities is more significant in the ASU. The main reasons are that the industrial development mode was relatively extensive, environmental protection awareness was insufficient, and the discharge of industrial wastewater may have significant impact on hydrochemistry during the initial stages of urbanization and industrial development. At this time, agricultural development was relatively slow, with less fertilizer application (average of 0.324 t/hm^2), and the impact of agricultural activities on groundwater chemistry was limited. Therefore, the impact of industrial activities on groundwater chemistry was greater than that of agricultural activities. During the ISU and ASU, due to government supervision and increased environmental awareness, the treatment and discharge of industrial pollutants were controlled to a certain extent, mitigating the impact of industrial emissions on groundwater chemistry. Thus, the content of SO_4^{2-} remained relatively stable. At the same time, agriculture is in a period of rapid development, and excessive agricultural fertilization (average application amounts of 0.742 t/hm^2 and 0.940 t/hm^2) leads to the infiltration of unused nitrogen fertilizer from plants into groundwater through agricultural irrigation or rainfall, leading to an increase in NO_3^- content in groundwater. It is manifested that over time, the increase rate of NO_3^- content is higher than that of SO_4^{2-} . Compared to the ISU, the NO_3^- content in the ASU was relatively stable, but the SO_4^{2-} content increased in some water samples. This may be due to intensified water–rock interactions (such as gypsum dissolution) related to groundwater over-extraction and industrial pollution [35].

4.4. Driving Mechanism for Temporal Evolution of Hydrochemistry

Groundwater chemistry evolution is influenced by a combination of various factors. In this study, PCA was used to identify the driving factors for hydrochemical evolution during the three urbanization stages in the study area. Eleven water quality parameters (pH, K^+ , Na^+ , Ca^{2+} , Mg^{2+} , Cl^- , SO_4^{2-} , HCO_3^- , NO_3^- , TDS, and TH) were selected for PCA analysis. Based on eigenvalues >1, two, two, and three main factors controlling water chemistry evolution in the PSU, ISU, and ASU were identified, explaining 74.4%, 69.9%, and 86.9% of all variables, respectively, representing all information from the eleven water chemistry indicators (Table 1).

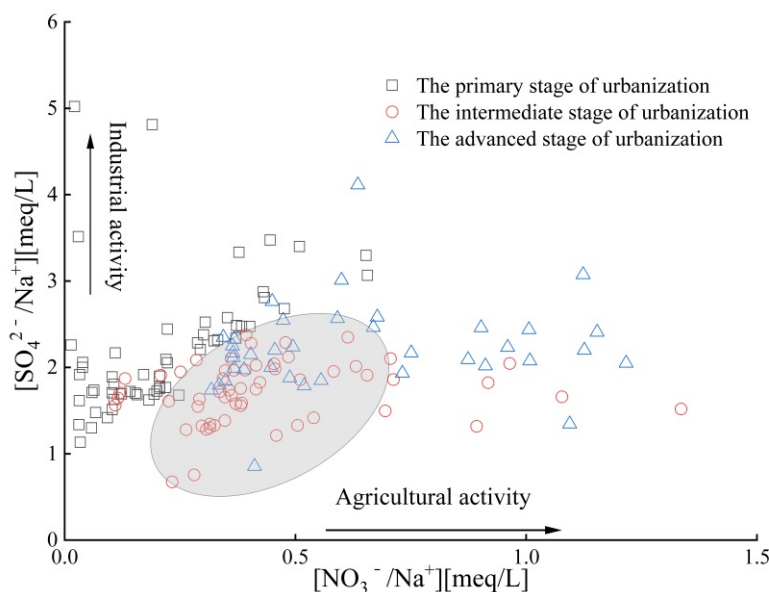


Figure 7. Variation relationship of $\text{SO}_4^{2-}/\text{Na}^+$ and $\text{NO}_3^-/\text{Na}^+$ in different stages of urbanization.

Table 1. PCA analysis results at each stage of urbanization.

Parameters	Primary Stage of Urbanization		Intermediate Stage of Urbanization		Advanced Stage of Urbanization		
	PC1	PC2	PC1	PC2	PC1	PC2	PC3
TDS	0.985	−0.089	0.957	0.106	0.272	0.708	0.511
Ca^{2+}	0.952	−0.205	0.925	−0.113	0.796	0.523	0.183
Mg^{2+}	0.922	−0.102	0.062	0.806	0.980	0.032	0.086
NO_3^-	0.882	−0.167	0.016	0.599	0.139	0.925	0.185
TH	0.868	0.011	0.870	0.013	0.834	0.331	0.227
SO_4^{2-}	0.868	0.061	0.934	−0.188	−0.074	0.243	0.916
HCO_3^-	0.859	−0.183	−0.401	0.646	0.036	0.851	0.239
Cl^-	0.612	−0.003	0.801	0.179	0.963	−0.052	−0.196
$\text{K}^+ + \text{Na}^+$	−0.039	0.827	0.765	0.014	0.744	−0.077	0.583
pH	−0.082	0.704	0.209	0.793	−0.045	−0.787	0.138
Eigenvalue	6.23	1.20	4.84	2.15	4.95	2.48	1.27
Contribution rate%	62.3	12.0	48.4	21.5	49.5	24.8	12.6
Cumulative contribution rate%	62.3	74.4	48.4	69.9	49.5	74.3	86.9

In the PSU, PC1 explained 62.4% of the total variable information, and the indicators exhibiting strong positive correlations with PC1 were TDS, Ca^{2+} , Mg^{2+} , NO_3^- , TH, SO_4^{2-} , and HCO_3^- , while Cl^- had a moderate positive correlation with PC1. As proven in Section 4.3.2, TDS, Ca^{2+} , Mg^{2+} , TH, HCO_3^- , and Cl^- were mainly related to carbonate dissolution. Previous studies have shown that NO_3^- in the water environment mainly comes from chemical fertilizers, sewage, manure, and soil nitrogen [36,37]. At this stage, the amount of agricultural fertilization is relatively small, the population density was low (230 people/ km^2), and the concentration of NO_3^- in groundwater was relatively low (mean value was 13.7 mg/L), indicating that the impact of agricultural activities on groundwater chemistry was limited. In addition, coal was the main fuel for industrial activities (mining activities, coking plants, power plants, etc.) in this period, and the sewage treatment capacity was relatively weak. Large amounts of discharged industrial wastewater will inevitably permeate into groundwater and lead to an increase in SO_4^{2-} concentration in groundwater [38]. Therefore, SO_4^{2-} in groundwater mainly originated from industrial activities. Thus, PC1 represents the control of groundwater chemistry by

carbonate dissolution and industrial activities. PC2 explained 12.0% of the total variable information, Na^+ and K^+ showed strong positive correlations with PC2, and pH displayed a moderate positive correlation. Based on previous analysis, Na^+ mainly originates from halite dissolution and cation exchange in the study area. The pH was influenced by various factors and did not have directionality, and the pH was relatively stable (7.20–8.15) during this period. Therefore, PC2 represents groundwater chemistry controlled by halite dissolution and cation exchange.

During the ISU, PC1 explained 62.4% of the total variable information, and indicators exhibiting strong positive correlations with PC1 included TDS, SO_4^{2-} , Ca^{2+} , and TH, while Cl^- and $\text{K}^+ + \text{Na}^+$ showed moderate positive correlations with PC1. Among them, TDS, SO_4^{2-} , Ca^{2+} , and TH were mainly related to carbonate and gypsum dissolution. As proven in Section 4.3.3, with the gradual implementation of government environmental protection policies, strict supervision of industrial non-compliant emissions has reduced the impact of industrial pollution on groundwater chemistry, and SO_4^{2-} concentration (151 mg/L) was relatively stable. Thus, PC1 represents that the groundwater chemistry was controlled by carbonate and gypsum dissolution. PC2 explained 21.5% of the total variable information. Mg^{2+} and pH showed strong positive correlations with PC2 and HCO_3^- and NO_3^- displayed moderate positive correlations. As known from Sections 4.3.2 and 4.3.3, this stage belongs to a period of rapid agricultural development, with increased groundwater extraction intensity and high fertilizer application (0.742 t/hm²). This not only affects water–rock interactions but also allows unutilized nitrogen fertilizers to infiltrate groundwater through irrigation return water and rainfall runoff [23]. The combined effect of these factors leads to an increase in Mg^{2+} , HCO_3^- , and NO_3^- concentrations. Additionally, livestock breeding and domestic sewage also affect groundwater chemistry. Therefore, PC2 represents that the groundwater chemistry was controlled by groundwater extraction intensity, agricultural fertilization, and domestic sewage.

In the ASU, PC1 explained 49.5% of the total variable information. Indicators showing a strong positive correlation with PC1 included Mg^{2+} , Cl^- , and TH, while Ca^{2+} and $\text{K}^+ + \text{Na}^+$ had a moderate positive correlation with PC1. Mg^{2+} , TH, and Ca^{2+} primarily originated from carbonate dissolution, while Cl^- and Na^+ mainly came from halite dissolution (as proven in Section 4.3.2). Therefore, PC1 represents the groundwater chemistry controlled by carbonate and halite dissolution. PC2 explained 24.8% of the total variable information. NO_3^- , HCO_3^- , and TDS showed a strong positive correlation with PC2, while pH had a moderate negative correlation. Section 4.3.3 has proven that high concentrations of NO_3^- primarily come from fertilizers and sewage during this stage. The negative correlation between HCO_3^- and pH indicated that decarbonation occurred in groundwater [39]. Under intense human exploitation of groundwater, water–rock interactions were enhanced, and the concentration of TDS was increased ultimately [40]. Therefore, PC2 represents that the groundwater chemistry was controlled by agricultural activities, sewage, and extraction intensity. The main factor PC3 explained 12.6% of the total variable information, and the indicator that showed a strong positive correlation with PC3 was SO_4^{2-} . In this period, the concentration of SO_4^{2-} was close to that of the previous period (180 mg/L and 190 mg/L, respectively), both originating from gypsum dissolution. Thus, PC3 represents that the groundwater hydrochemistry was controlled by gypsum dissolution.

5. Conclusions

This study is the first to identify the characteristics and driving mechanisms of groundwater chemistry evolution at different urbanization stages in the world. The results showed that with the acceleration of urbanization, the concentration of various groundwater chemical components gradually increases, especially NO_3^- , which has risen from 13.7 mg/L in the primary stage of urbanization (PSU) to 65.1 mg/L, exceeding the World Health Organization (WHO) drinking water standard (50 mg/L), indicating that groundwater chemistry was significantly influenced by human activities. The hydrochemical type changed from $\text{HCO}_3\text{-SO}_4\text{-Ca}\cdot\text{Mg}$ in the PSU to $\text{SO}_4\cdot\text{HCO}_3\text{-Ca}\cdot\text{Mg}$ in the advanced stage of urbanization

(ASU). Groundwater chemical processes have shifted from being primarily controlled by dissolution and filtration in the PSU to joint control by dissolution, filtration, and human activities in the ASU. Based on PCA analysis, the driving factors for groundwater chemistry evolution were identified. In the PSU, the driving factors of groundwater chemical evolution were carbonate and rock salt dissolution, cation exchange, and industrial activities. However, in the intermediate stage and advanced stage, the driving factors were changed to carbonate and gypsum dissolution, groundwater over-exploitation, agricultural fertilization, and domestic sewage. Based on these conclusions, we recommend controlling the amount of agricultural fertilization, scientific fertilization, and prohibiting non-compliant sewage discharge in future groundwater management. Additionally, supervision of groundwater extraction should be strengthened to reduce the impact of urbanization on groundwater chemistry evolution.

Supplementary Materials: The following are available online at <https://www.mdpi.com/article/10.3390/w15162917/s1>, Table S1: Statistics of water sample index in each urbanization stage.; Table S2: Statistical of water sample index in each urbanization stage.

Author Contributions: L.W.: Investigation, Methodology, Software, Data curation, Writing—Original Author Contributions, Draft Preparation. Q.Z.: Supervision, Methodology, Writing—Reviewing and Editing. H.W.: Investigation, Software, Supervision. All authors have read and agreed to the published version of the manuscript.

Funding: This work was supported by the open funds of Natural Science Foundation of Hebei Province of China (Grant No. D2022504015), the Fundamental Research Funds for the Chinese Academy of Geological Sciences (No. YK202310), the Projects of China Geological Survey, China (Grant No. DD20221773-2) and the High-level talent funding project of Hebei Province, China (Grant No. A202101003).

Data Availability Statement: The data are available from the authors upon reasonable request.

Acknowledgments: The authors gratefully acknowledge the editor and anonymous reviewers for their valuable comments on this manuscript. The authors also appreciate the financial support from the different organizations.

Conflicts of Interest: The authors declare no conflict of interest.

References

1. Li, P.; Karunanidhi, D.; Subramani, T.; Srinivasamoorthy, K. Sources and Consequences of Groundwater Contamination. *Arch. Environ. Con. Tox.* **2021**, *80*, 1–10.
2. Pashaeifar, M.; Dehghanzadeh, R.; Ramazani, M.E.; Rafieyan, O.; Nejaei, A. Spatial and temporal assessment of groundwater quality and hydrogeochemical processes in Urmia Lake Basin, Iran. *Water Supply* **2021**, *21*, 4328–4342. [[CrossRef](#)]
3. Peng, H.; Yang, W.; Ferrer, A.; Xiong, S.; Li, X.; Niu, G.; Lu, T. Hydrochemical characteristics and health risk assessment of groundwater in karst areas of southwest China: A case study of Bama, Guangxi. *J. Clean. Prod.* **2022**, *341*, 130872.
4. Quinn, N.W.T.; Oster, J.D. Innovations in Sustainable Groundwater and Salinity Management in California’s San Joaquin Valley. *Sustainability* **2021**, *13*, 6658. [[CrossRef](#)]
5. Saccò, M.; Blyth, A.; Douglas, G.; Humphreys, W.; Hose, G.; Davis, J.; Guzik, M.; Martínez, A.; Nez, A.; Eberhard, S.; et al. Stygofaunal diversity and ecological sustainability of coastal groundwater ecosystems in a changing climate: The Australian paradigm. *Freshw. Biol.* **2022**, *67*, 2007–2023.
6. Qin, R.; Song, Q.; Hao, Y.; Wu, G. Groundwater level declines in Tianjin, North China: Climatic variations and human activities. *Environ. Dev. Sustain.* **2022**, *25*, 1899–1913. [[CrossRef](#)]
7. Akakuru, O.; Eze, C.; Okeke, O.; Opara, A.I.; Usman, A.O.; Iheme, O.; Ibeneme, S.I.; Iwuoha, P.O. Hydrogeochemical evolution, water quality indices, irrigation suitability and pollution index of groundwater pig around Eastern Niger Delta, Nigeria. *Int. J. Energy Res.* **2022**, *6*, 389–411.
8. Israr, M.; Nazneen, S.; Raza, A.; Ali, N.; Khan, S.A.; Khan, H.; Khan, S.; Ali, J. Assessment of municipal solid waste landfilling practices on the groundwater quality and associated health risks: A case study of mar-dan-pakistan. *Arab. J. Geosci.* **2022**, *15*, 1445.
9. Kai, L.; Zhong, P.; Raza, A. Impact of rapid urbanization on water quality index in groundwater fed Gomati River, Lucknow, India. *Curr. Sci.* **2018**, *3*, 650–654.
10. Liu, J.; Yang, H.; Gosling, S.N.; Kummu, M.; Flörke, M.; Pfister, S.; Hanasaki, N.; Wada, Y.; Zhang, X.; Zheng, C.; et al. Water scarcity assessments in the past, present, and future. *Earth’s Future* **2017**, *5*, 545–559. [[CrossRef](#)]

11. Huang, G.; Sun, J.; Zhang, Y.; Chen, Z.; Liu, F. Impact of anthropogenic and natural processes on the evolution of groundwater chemistry in a rapidly urbanized coastal area, South China. *Sci. Total Environ.* **2013**, *463*, 209–221. [[CrossRef](#)]
12. Olds, H.T.; Corsi, S.R.; Dila, D.K.; Halmo, K.M.; Bootsma, M.J.; McLellan, S.L. High levels of sewage contamination released from urban areas after storm events: A quantitative survey with sewage specific bacterial indicators. *PLoS Med.* **2018**, *15*, e1002614.
13. Barron, O.V.; Barr, A.D.; Donn, M.J. Evolution of nutrient export under urban development in areas affected by shallow watertable. *Sci. Total Environ.* **2013**, *443*, 491–504. [[CrossRef](#)]
14. Zhang, Q.; Wang, H. Assessment of sources and transformation of nitrate in the alluvial-pluvial fan region of north China using a multi-isotope approach. *J. Environ. Sci.* **2020**, *3*, 9–22. [[CrossRef](#)]
15. Rai, S.C.; Saha, A.K. Impact of urban sprawl on groundwater quality: A case study of Faridabad city, National Capital Region of Delhi. *Arab. J. Geosci.* **2015**, *8*, 8039–8045. [[CrossRef](#)]
16. Villegas, P.; Paredes, V.; Betancur, T.; Ribeiro, L. Assessing the hydrochemistry of the urabá aquifer, Colombia by principal component analysis. *J. Geochem. Explor.* **2013**, *134*, 120–129.
17. Sinha, R.; Elango, L. Deterioration of groundwater quality: Implications and management. In *Water Governance: Challenges and Prospects*; Springer: Singapore, 2019; pp. 87–101.
18. Huang, Z.; Pan, Y.; Gong, H.; Yeh, P.J.F.; Li, X.; Zhou, D.; Zhao, W. Subregional-scale groundwater depletion detected by GRACE for both shallow and deep aquifers in North China Plain. *Geophys. Res. Lett.* **2015**, *42*, 1791–1799. [[CrossRef](#)]
19. Zheng, C.; Liu, J.; Cao, G.; Kendy, E.; Wang, H.; Jia, Y. Can China Cope with Its Water Crisis?—Perspectives from the North China Plain. *Groundwater* **2010**, *48*, 350–354. [[CrossRef](#)]
20. Ren, C.; Zhang, Q.; Wang, H.; Wang, Y. Characteristics and source apportionment of polycyclic aromatic hydrocarbons of groundwater in Hutuo river alluvial-pluvial fan, China, based on PMF model. *Environ. Sci. Pollut. R.* **2021**, *28*, 9647–9656.
21. GB/T8538-2008; General Administration of Quality Supervision, Inspection and Quarantine of the People's Republic of China, Methods for Examination of Drinking Natural Mineral Water. Standards Press of China: Beijing, China, 2008. (In Chinese)
22. Zhang, Q.; Wang, X.; Wan, W.; Hou, P.Q.; Li, R.; Ouyang, Z. The Spatial-Temporal Pattern and Source Apportionment of Water Pollution in a Trans-Urban River. *Pol. J. Environ. Stud.* **2015**, *24*, 841–851.
23. Zhang, Q.; Wang, H.; Wang, Y.; Yang, M.; Zhu, L. Groundwater quality assessment and pollution source apportionment in an intensely exploited region of northern China. *Environ. Sci. Pollut. R.* **2017**, *24*, 16639–16650.
24. Chen, R.; Hu, Q.; Shen, W.; Guo, J.; Yang, L.; Yuan, Q.; Lu, X.; Wang, L. Identification of nitrate sources of groundwater and rivers in complex urban environments based on isotopic and hydro-chemical evidence. *Sci. Total Environ.* **2023**, *871*, 162026. [[CrossRef](#)] [[PubMed](#)]
25. Yang, J.; Ye, M.; Tang, Z.; Tian, J.; Xiaoyu, S.; Yongzhen, P.; Honghua, L. Using cluster analysis for understanding spatial and temporal patterns and controlling factors of groundwater geochemistry in a regional aquifer. *J. Hydrol.* **2020**, *583*, 124594.
26. World Health Organization. *Guidelines for Drinking-Water Quality*, 4th ed.; World Health Organization: Geneva, Switzerland, 2011.
27. Fei, L.; Jza, B.; Jza, B.; Pza, B. Factors controlling groundwater chemical evolution with the impact of reduced exploitation. *Catena* **2022**, *214*, 106261.
28. Mukate, S.; Bhoominathan, S.; Solanky, V. Assessment of human health risk arising due to fluoride and nitrate in groundwater: A case study of Bhokardan tehsil of Maharashtra. *Hum. Ecol. Risk Assess. Int. J.* **2022**, *28*, 594–620. [[CrossRef](#)]
29. Hasan, M.S.U.; Rai, A.K. Groundwater quality assessment in the Lower Ganga Basin using entropy information theory and GIS. *J. Clean. Prod.* **2020**, *274*, 123077. [[CrossRef](#)]
30. Tiwari, A.K.; Singh, A.K.; Singh, A.K.; Singh, M.P. Hydrogeochemical analysis and evaluation of surface water quality of Pratapgarh district, Uttarpradesh, India. *Appl. Water Sci.* **2017**, *7*, 1609–1623.
31. Wang, Q.; Dong, S.; Wang, H.; Yang, J.; Yu, B. Hydrogeochemical processes and groundwater quality assessment for different aquifers in the Caojatan coal mine of Ordos Basin, northwestern China. *Environ. Earth Sci.* **2020**, *79*, 199.
32. Xiaohui, R.; Zhang, Z.; Yu, R.; Li, Y.; Li, Y.; Zhao, Y. Hydrochemical variations and driving mechanisms in a large linked river-irrigation-lake system. *Environ. Res.* **2023**, *225*, 115596.
33. Li, Y.; Zhang, Z.; Fei, Y.; Chen, H.; Qian, Y.; Yu, D. Investigation of quality and pollution characteristics of groundwater in the Hutuo River alluvial plain, North China plain. *Environ. Earth Sci.* **2016**, *75*, 581.
34. Lü, X.; Liu, J.; Han, Z.; Zhu, L.; Chen, X. Effects of Yindaruqin irrigation project on groundwater chemical compositions in Qinwangchuan basin in Gansu Province Article. *Trans. Chin. Soc. Agric. Eng.* **2020**, *36*, 166–174. (In Chinese)
35. Torres-Martínez, J.A.; Mora, A.; Knappett, P.S.K.; Ornelas-Soto, N.; Mahlkecht, J. Tracking nitrate and sulfate sources in groundwater of an urbanized valley using a multi-tracer approach combined with a Bayesian isotope mixing model. *Water Res.* **2020**, *182*, 115962. [[PubMed](#)]
36. Panda, B.; Chidambaram, S.; Snow, D.; Malakar, A.; Singh, D.K.; Ramanathan, A.L. Source apportionment and health risk assessment of nitrate in foothill aquifers of Western Ghats, South India. *Ecotoxicol. Environ. Saf.* **2021**, *229*, 113075. [[CrossRef](#)] [[PubMed](#)]
37. Zhang, Q.; Shu, W.; Li, F.; Li, M.; Zhou, J.; Tian, C.; Liu, S.; Ren, F.; Chen, G. Nitrate source apportionment and risk assessment: A study in the largest ion-adsorption rare earth mine in China. *Environ. Pollut.* **2022**, *302*, 119052. [[CrossRef](#)] [[PubMed](#)]
38. Torres-Martínez, J.A.; Mora, A.; Mahlkecht, J.; Kaown, D.; Barceló, D. Determining nitrate and sulfate pollution sources and transformations in a coastal aquifer impacted by seawater intrusion—A multi-isotopic approach combined with self-organizing maps and a Bayesian mixing model. *J. Hazard. Mater.* **2021**, *417*, 126103. [[CrossRef](#)]

39. Yu, B.; Lai, X. Carbonic Acid System of Groundwater and the Solubility of Calcite during Diagenesis. *Acta Sed. Sin.* **2010**, *24*, 627–635. (In Chinese)
40. Zhou, B.; Wang, H.; Zhang, Q. Assessment of the Evolution of Groundwater Chemistry and Its Controlling Factors in the Huangshui River Basin of Northwestern China, Using Hydrochemistry and Multivariate Statistical Techniques. *Int. J. Environ. Res. Public Health* **2021**, *18*, 7551. [[CrossRef](#)]

Disclaimer/Publisher’s Note: The statements, opinions and data contained in all publications are solely those of the individual author(s) and contributor(s) and not of MDPI and/or the editor(s). MDPI and/or the editor(s) disclaim responsibility for any injury to people or property resulting from any ideas, methods, instructions or products referred to in the content.